





## Thermal Impact on the Physical and Transfer Properties of Slag Cement and Portland Cement Concretes

Cheikh Zemri<sup>1,2\*</sup> , Mohamed Bachir Bouiadjra<sup>3</sup> 

<sup>1</sup> Department of Civil Engineering, Mustapha Stambouli University, Mascara 29000, Algeria

<sup>2</sup> Civil and Environmental Engineering Laboratory, Djilali Liabes University, Sidi Bel-Abbes 22000, Algeria

<sup>3</sup> Advanced Materials and Structures in Civil Engineering and Public Works, Djilali Liabes University, Sidi Bel-Abbes 22000, Algeria

Corresponding Author Email: [ch.zemri@univ-mascara.dz](mailto:ch.zemri@univ-mascara.dz)

Copyright: ©2023 IIETA. This article is published by IIETA and is licensed under the CC BY 4.0 license (<http://creativecommons.org/licenses/by/4.0/>).

<https://doi.org/10.18280/acsm.470603>

### ABSTRACT

**Received:** 27 July 2023

**Revised:** 3 October 2023

**Accepted:** 15 October 2023

**Available online:** 22 December 2023

#### Keywords:

*high temperature, concrete durability, slag cement, Portland cement, diffusivity, porosity, permeability*

The cement industry confronts significant environmental challenges, primarily due to extensive raw material and energy consumption, and consequential substantial greenhouse gas emissions such as carbon dioxide. Escalating energy expenses and stringent environmental regulations mandate the reduction of industrial emissions through the incorporation of industrial by-products like blast furnace slag. In this study, a comparative analysis was conducted to evaluate the physical and transport properties of concrete made with slag cement versus that made with Portland cement, particularly after exposure to high-temperature conditions. Specimens, cured for 90 days at 20°C in water, underwent a series of four heating-cooling cycles at incremental temperatures of 160, 300, 400, and 650°C, with a consistent heating rate of 1°C/min. Various durability indicators, including mass loss, water-accessible porosity, gas permeability, capillary water absorption coefficient, and chloride ion apparent diffusion coefficient, were measured. It was observed that an increase in the temperature of exposure led to a reduction in weight, porosity, permeability, diffusivity, and capillary water absorption in both concrete types. Notably, the slag cement concrete exhibited marginally superior durability parameters compared to the Portland cement concrete, with the exception of porosity. Empirical correlations derived from the experimental data between porosity, water absorption, and gas permeability facilitate the assessment of the apparent diffusion coefficient in fire-damaged concrete incorporating blast furnace slag, up to a temperature of 650°C.

## 1. INTRODUCTION

Investigations into the influence of high temperatures on concrete's mechanical properties commenced in the early 1940s [1]. It is universally recognized that fire can inflict damage on concrete via two primary mechanisms. Initially, the constrained thermal expansion induces compressive stresses parallel to the heated surface, engendering tensile stresses in the orthogonal direction [2]. Concurrently, the increase in pore pressure within the concrete, attributable to the vaporization of both physically and chemically bound water, exerts a tensile force upon the microstructure [3]. Contemporary research [4-11] has elucidated that exposure to elevated temperatures can precipitate a diminution in both the mechanical strength and durability of concrete, thereby compromising the integrity of fire-damaged structures. Notably, the manifestation of cracks under such thermal duress could deteriorate the durability of concrete edifices by establishing preferential channels that expedite the ingress of deleterious agents, including liquids, gases, and ions [12].

The presence of chloride ions is particularly detrimental to

the longevity of reinforced concrete structures, as they are capable of inflicting severe harm, especially in coastal, marine, or salt-exposed infrastructures [13]. Frequently, such structures incorporate cementitious materials derived from blast furnace slag [14], which, over time, tend to exhibit fine capillary porosity [15-18], a reduced permeability coefficient [17, 19], and a diminished chloride diffusion coefficient in cement pastes [20, 21], mortars [22, 23], and concrete [24, 25]. Moreover, blast furnace slag provides multifaceted advantages, including the valorization of industrial by-products, the mitigation of CO<sub>2</sub> emissions during the clinkerization process [26, 27], the augmentation of workability [28-30], and the enhancement of compressive strength over extended durations [29-32].

Blast furnace slag, a by-product of the steel industry, is produced during the smelting of iron ore, coke, and fluxes, which is essential for cast iron preparation. Harvested from the blast furnace at temperatures between 1300°C and 1600°C [33], it is estimated that the production of one ton of cast iron may yield approximately 300 kg of slag [34]. The chemical composition of slag, predominantly consisting of CaO, SiO<sub>2</sub>,

Al<sub>2</sub>O<sub>3</sub>, MgO, and FeO, shares similarities with the oxides found in ordinary Portland cement, albeit in differing ratios [34]. These compositional traits bestow upon slag certain hydraulic characteristics, although its hydration necessitates activation by either calcium or alkalis. Such activation is commonly achieved through portlandite from hydrated clinker or by calcium sulfate from gypsum, especially in the presence of Portland cement [35, 36]. Slag cement (CEM III) is produced in cement plants by substituting a significant portion of clinker—ranging from 36% to 95%—with slag [37].

In recent years, the scholarly focus has been placed on the impact of blast furnace slag on the diffusion of chloride ions within cementitious materials [4, 38–40] prior to fire exposure. Despite these efforts, the post-fire behavior of chloride ion diffusion in such materials remains underexplored. In response to this research void, the present study endeavors to critically evaluate and contrast the durability, gas permeability, and chloride ion diffusivity of CEMIII and CEMI concretes subsequent to fire exposure.

## 2. EXPERIMENTAL PROTOCOLS

### 2.1 Materials used

The present study was carried out on two distinct concretes prepared with two different types of cement. The first concrete (BI) was based on Portland cement (CEM I 52.5 N), and the second one (BIII) contained blast furnace cement (CEM III / A 52.5 N). In addition, the Blaine fineness of the two types of cement was respectively equal to 3650 cm<sup>2</sup>/g and 4263 cm<sup>2</sup>/g. And their specific gravity was 3.15 and 2.98, respectively. Moreover, their respective physicochemical compositions and mineralogical are given in Tables 1 and 2.

**Table 1.** Elemental chemical composition of the cements (%)

	CEMI	CEMIII
CaO	64.53	49.90
SiO <sub>2</sub>	20.12	29.10
Al <sub>2</sub> O <sub>3</sub>	05.03	08.50
Fe <sub>2</sub> O <sub>3</sub>	03.12	01.00
SO <sub>3</sub>	00.98	05.00
K <sub>2</sub> O	00.98	00.32
Na <sub>2</sub> O	00.16	00.40
MgO	03.34	02.67

**Table 2.** Mineralogical composition of the cements (%)

	C <sub>3</sub> S	C <sub>2</sub> S	C <sub>3</sub> A	C <sub>4</sub> AF
CEM I	63.90	12.60	08.09	09.80
CEM III	62.00	14.00	12.00	06.00

**Table 3.** Formulation of ordinary concrete (Kg/m<sup>3</sup>)

	BI	BIII
Sand 0/4	710	685
Gravel 6.3/10	365	360
Gravel 10/20	725	715
Cement	400	400
Water	200	200

The granular skeleton was composed of fine aggregates (sand) which generally contain quartz, and coarse aggregates (gravel) which is mainly composed of silica and quartz. In addition, it should also be noted that, before mixing, the sand

and gravel were previously dried in an oven at 60°C, for two days, in order to remove excess water. Then, this sand was screened according to a sieving process to obtain a particle gradation of 0/4 with a density of 2.6 and a water absorption coefficient of 1.2%. Likewise, the aggregates were sieved separately in order to obtain two more granular classes (6.3/10 and 10/20) with a density of 2.66 and a water absorption coefficient of 0.5%. Table 3 shows the compositions of the concretes used, for water-to-cement (W/C) ratio equal to 0.5 and a sand-to-cement (S/C) ratio equal to 1.775.

Once the concrete was mixed, it was poured into waxed cardboard cylinder molds 11 cm in diameter and 22 cm in height. After 24 hours, the test pieces were removed from the molds and stored in water for 90 days in a humid room.

### 2.2 Heat treatment

Once they were hardened for 90 days in a humid chamber the specimens of dimensions (110 × 220) mm<sup>2</sup> were sawn into cylindrical slices of diameter 110 mm and thickness 60 mm; they were then dried in an oven at 60°C until mass stabilization. It should be mentioned that 60°C was chosen as the initial reference temperature for all the performed tests, in order to characterize the undamaged or healthy material. Afterwards, the concrete samples were heated in a Nabertherm electric furnace that was successively set to the temperatures of 160, 300, 400 and 650°C. The heating rate was set at 1°C/min., and each temperature was kept constant for 1 hour in order to reach a thermally stable state. The temperature rises and fall rates were chosen in accordance with the recommendations of the RILEM technical committee TC-129 [41].

### 2.3 Porosity test

The porosity accessible to water was determined in accordance with the recommendations of the AFREM group [42]—which predicts the saturation of the samples in single-phase mode (under vacuum). The tests were carried out on cylindrical samples 40 mm in diameter and 60 mm in height— which were cored on specimens of dimensions (110 × 60) mm<sup>2</sup>. The samples were then placed under a vacuum bell for 24 hours. Afterwards, they were immersed in water, and then kept under vacuum for 48 hours. It is worth indicating that the sample volume was determined by weighing it in air and then in water using a hydrostatic weighing device. Then, in order to obtain the dry mass, the samples were dried at 60°C until a constant mass was reached. The porosity accessible to water could then be calculated using the following formula:

$$\varepsilon = \frac{M_{air} - M_{dry}}{M_{air} - M_{water}} \rho_{water} \quad (1)$$

where,  $M_{air}$  is the mass of the sample saturated in air,  $M_{water}$  is the mass of the sample saturated in water, and  $M_{dry}$  is the mass of the sample at the end of drying.

### 2.4 Gas permeability test

The gas permeability measurements were carried out using a permeameter at constant load, in accordance with the recommendations of RILEM [43] and in conformity with the method of Cembureau [44]. The gas used in this study was helium. The principle of the test was to maintain a constant gas pressure difference between the two ends of the sample, and

to measure the resulting flow when steady state was reached. The experimental setup is shown in Figure 1.

The sample of dimensions (110 × 60) mm<sup>2</sup> was then placed in the cell for measuring the permeability of concrete to gas. In this test, a toric airchamber was inflated to a pressure of 8 bars and compressed the sample holder to ensure lateral sealing. The percolation gas  $P_1$  (absolute pressure of 2 bars) was then injected through the upper face of the cell. At the cell outlet, the gas flow was measured using a mass flow meter that was placed in direct contact with the outlet pressure  $P_0$  that is equal to the atmospheric pressure (absolute pressure of 1 bar).

Furthermore, the apparent permeability coefficient ( $K_a$ ) was calculated for the laminar flow of a viscous compressible fluid through a porous material applying the Hagen-Poiseuille relationship [44].

$$k_a = \frac{2\mu Q P_1 L}{A(P_1^2 - P_0^2)} \quad (2)$$

where,  $Q$  is the measured gas flow rate (m<sup>3</sup>/s),  $\mu$  is the dynamic viscosity of helium (Ns/m<sup>2</sup>),  $L$  is the thickness of the sample (m),  $P_0$  the atmospheric pressure (Pa),  $A$  the cross section of the sample (m<sup>2</sup>), and  $P_1$  the applied absolute pressure (Pa).

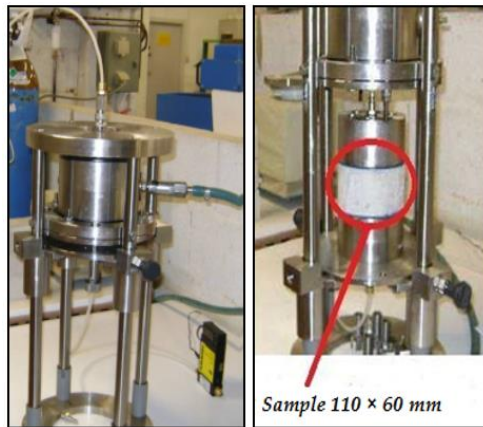


Figure 1. Experimental device for measuring the permeability

## 2.5 Water absorption test



Figure 2. Capillary water absorption tests

With regard to the capillary water absorption assessment, it was decided to adopt a test that is generally applied to mortar. This test was indeed conducted on cylindrical concrete samples 40 mm in diameter and 60 mm in height. Its principle consisted of placing one end face of the sample at a depth of 1 cm in a body of water maintained at a constant level, and then

measuring the weight gain values of the sample at well-defined time intervals. The side faces were waterproofed by molten paraffin wax beforehand [45], which forced water to adopt a uniaxial path and to prevent the evaporation of water from these faces. Obviously, the sheet of water retained on the underside of the sample had to be carefully removed before each weighing using absorbent paper. Figure 2 illustrates the experimental setup.

The amount of water absorbed per unit area after one hour was used as a quantity that represents the volume of the largest capillaries present in the skin area [46].

## 2.6 Chloride ion diffusion test

The cylindrical concrete specimens, 110 mm in diameter and 60 mm in height, were saturated with 0.1 M NaOH solution under vacuum, for 24 hours, before starting the diffusion test. This solution was selected because the higher the pH of the solution, the less the chloride ions were fixed [47], which maximized the penetration of free chlorides into concrete. The surfaces of the samples were covered with an adhesive aluminum foil, except for the sawn surface that was intended for contact with the NaCl solution (a mixture of 0.51M NaCl and 0.1M NaOH). The test pieces were then partially immersed into the above-mentioned solution for 60 days, as illustrated in Figure 3. It should be noted that, during the test, the test pieces and the solution were kept in a closed tank in order to limit the evaporation of water.

The depth of penetration of the chloride ions could then be obtained by spraying a 0.1 M silver nitrate solution on the faces obtained after splitting the specimen [48]. The AgNO<sub>3</sub> solution revealed, by color difference, the interface between the healthy zone and the zone containing chloride ions. The values of chloride penetration depth could then be used to calculate the apparent diffusion coefficient in accordance with the formula proposed by Baroghel-Bouny et al. [49] as given below:

$$D_{ns(dif)} = \frac{X_d^2}{4t} \quad (3)$$

where,  $D_{ns(dif)}$  is the apparent diffusion coefficient of chloride ions under saturation conditions (m<sup>2</sup>/s),  $X_d$  is the penetration depth of chloride ions (m), and  $t$  is the immersion time of test pieces into the solution (s).

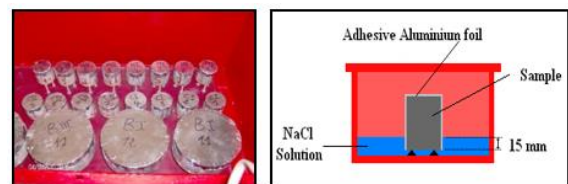


Figure 3. Chloride ion diffusion test in transient regime

## 3. RESULTS AND INTERPRETATION

### 3.1 Loss of mass

The mass loss of the concrete specimens, following their exposure to high temperatures, was evaluated by measuring the mass of these specimens before and after exposure to fire. The percentage changes in mass, at different temperatures,

were calculated and are presented in Figure 4. It is worth specifying that the average experimental results obtained for each sample as well as the error bars are simultaneously presented in order to make a visual comparison between the uncertainties in the measurements performed. It was therefore found that the mass loss of all concretes (BI and BIII) gradually increased from 3.16 % to 8.72 % when the temperature increased from 160 to 650°C. According to Kalifa [50], the loss of mass of concrete before 600°C was mainly attributed to the departure of water. In addition, it was also noticed that the mass losses of concretes containing blast furnace slag cement (BIII) were slightly greater than those of Portland cement concretes (BI), except for the heating temperature equal to 160°C.

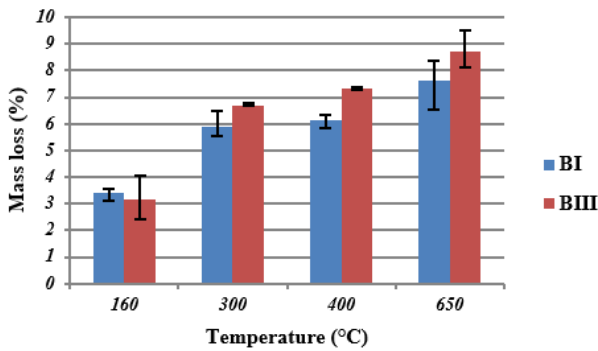


**Figure 4.** Mass loss of concrete samples under the effect of temperature

It is worth mentioning that between room temperature and 160°C, a small loss of mass, due to the departure of free water, capillary water [51] and to the decomposition of ettringite [52], was recorded. It should also be noted that the mass loss of concrete BIII (3.16 %) was lower than that of concrete BI (3.40 %), which could be explained by the pozzolanic reaction, in the presence of blast furnace slag in cement CEM III. This reaction consumes Portlandite as well as free water to form additional calcium silicate hydrates (CSHs) [53]. Therefore, there will be less free water to evaporate from the structure of concrete BIII than from that of concrete BI. Another explanation is due to the low ettringite content after cement hydration in the presence of blast furnace slag, in accordance with the Lothenbach model [54].

Furthermore, at the temperatures of 300°C, 400°C and 650°C, the mass losses increased rapidly. This was mainly due, firstly, to the departure of water initially contained in the calcium silicate hydrates (CSHs), to the decomposition of these hydrates [55] and portlandite  $\text{Ca}(\text{OH})_2$ , between temperatures 450°C and 550°C, to give calcium oxide (CaO) and water ( $\text{H}_2\text{O}$ ) [51] that evaporate, and secondly to the dehydration of the CSHs between the temperatures 600°C and 700°C [56]. When subjected to the temperatures of 300, 400 and 650°C, the mass losses of concretes BIII were found respectively equal to 6.7 %, 7.31 % and 8.72 %. As is seen, these results are slightly greater than those observed for concrete BI for which they were respectively equal to 5.9 %, 6.14 % and 7.61 %. This can certainly be assigned to the higher CSH content of slag concretes (BIII). Similar results were reported by Khan and Abbas [39] who concluded that the loss of mass from concrete to blast furnace slags increases sharply with increasing temperature up to 700°C.

With regard to Li et al. [38], they indicated that the mass losses of blast furnace slag concretes exposed to high

temperatures, between 150°C and 700°C, were less than 8 % for temperatures below 700°C, while they were slightly higher than those of Portland cement concretes.

### 3.2 Porosity

Concrete is a two-phase porous material; it has a solid phase and a porous phase. It is well known that it is possible to characterize the porous network of concretes subjected to high temperatures by measuring their porosity. Figure 5 shows the evolution of the porosity accessible to water of concrete samples (BI) containing Portland cement and concrete samples (BIII) including blast furnace slag cement as a function of temperature. It was noted that at the reference temperature (60°C) the porosity of concrete (BIII) was slightly higher than that of concrete (BI). This increase in porosity was probably due to blast furnace slag consuming the non-porous portlandite to produce porous calcium silicate hydrates. Similar results were also observed in concrete in the study previously conducted by Divet and Roy [57] and in mortars in the work antecedently carried out by Bur [16].

It is worth indicating that when the temperature rises, the porosity of concrete (BI) increased by 3.5 % and 19.8 %, respectively, for the temperatures 160°C and 650°C. On the other hand, it decreased by 1.4 % and 4.3 % for the temperatures 300°C and 400°C, respectively. According to Kalifa [50] who studied ordinary concrete, and Piasta [58], who investigated cement pastes, the decrease in porosity within the temperature interval [300 - 400°C], was associated with densification that was due to the additional hydration and carbonation of portlandite under internal autoclaving conditions. In this case, the pressure is greater than the atmospheric pressure.

One could clearly see that for concretes (BIII), the variation of porosity with temperature followed a linear curve. Indeed, the porosity increased by 4.2 %, 6.6 %, 10.5 % and 20.3 %, respectively, for the temperatures 160°C, 300°C, 400°C and 650°C. The porosity increase was mainly due to the departure of the adsorbed water in the capillary pores and the bound water of hydrates present in the cement paste [51-53, 55, 56], as well as to the microcracking caused by the differential expansion occurring between paste and aggregates [7, 59].

Unlike in concrete (BI), hydrate densification was not observable in the case of concrete (BIII) which contains very little portlandite that was consumed during the pozzolanic reaction in the presence of blast furnace slag [4].

In addition, it was also noted that for each temperature, the porosity of concretes (BIII) was slightly higher than that of concretes (BI).

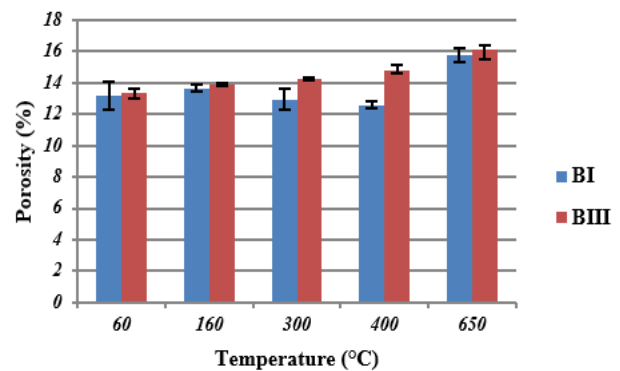


**Figure 5.** Effect of temperature on the porosity of concrete



### 3.3 Permeability

Permeability is defined as the ability of a material to pass a fluid. It generally reflects the significance, connectivity and tortuosity of the porous network. Figures 6 and 7 illustrate, respectively, the effects of temperature on the apparent permeability and relative permeability (ratio between reference permeability and initial permeability) of concretes (BI) and (BIII). Figure 6 clearly indicates that the apparent permeability of concrete increases with temperature in an exponential manner. A similar behavior has previously been found by Sliwinski [60] in the study he conducted on concrete including basalt aggregates heated at a rate of 1°C/min and cooled to room temperature.

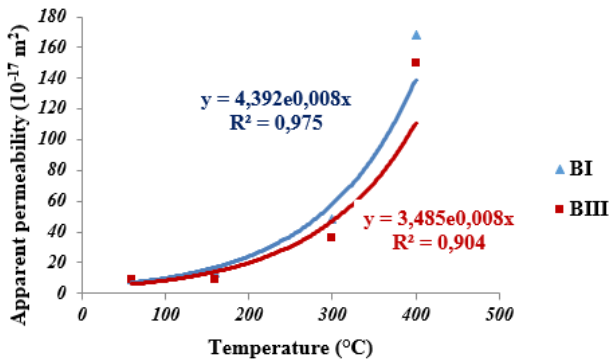


Figure 6. Effect of temperature on the apparent permeability of concrete

It should be noted that for both types of concrete (BI and BIII), the apparent permeability increased slightly when the temperature went from 60 to 160°C. Then, it continued to increase but more rapidly when the temperature increased from 160 to 300°C; this increase was even more significant between 300 and 400°C. These apparent permeability changes could be attributed to several factors [59, 61], namely the withdrawal of capillary water through drying, thermal microcracking caused by the dehydration of calcium-silicate-hydrates, and finally the incompatibility of thermal deformation between cement paste and the aggregates. The mass flow meter available in the laboratory (of capacity limited to 500 ml/min) could not measure the flow rate of the flow gas released in the samples of concrete heated to 650°C, the reason why the results of the apparent permeability and relative permeability have not shown, respectively, in Figures 6 and 7.

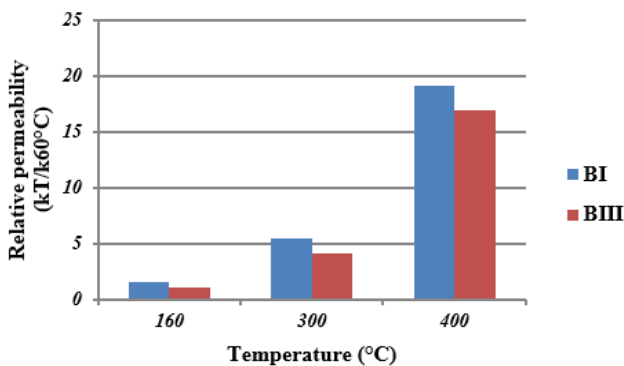


Figure 7. Effect of temperature on the relative permeability of concrete

Figure 7 explicitly shows that the change rate in concrete permeability with temperature is lower in the case of concrete including blast furnace slag cement (CEMIII) in comparison with that of concrete incorporating Portland cement (CEMI). Indeed, at the temperatures 160, 300 and 400°C, concretes (BIII) exhibited, respectively, the permeability growth rates of 1.04 %, 4.14 % and 16.94 % with respect to those observed in reference concrete (60°C). However, these permeability growth rates were respectively equal to 1.56 %, 5.47 % and 19.17 % for concrete (BI).

At the reference temperature (60°C), the apparent permeability of concrete (BIII) was slightly higher than that of concrete (BI). It was revealed that the permeability of concrete depends mainly on its capillary porosity. In addition, the previously found porosity data support well the permeability results obtained. Similar results on the gas permeability of concrete, for a replacement rate of 60 % of cement by blast furnace slag, have previously been reported by Hui-Sheng [62].

However, for the other temperatures (160, 300 and 400°C), the apparent permeabilities of concretes (BIII) were always lower than that of concrete (BI).

Furthermore, between 30°C and 120°C, the free water and part of the adsorbed water escaped from concrete, thus creating the passage for the percolating fluid. It was also revealed that the presence of blast furnace slag in CEM III cement promoted the pozzolanic reaction, which decreased the proportion of Portlandite and free water, to eventually form additional calcium silicate hydrates (CSHs) [4]. The amount of free water in the structure of concrete (BIII) was smaller than that in concrete (BI). Moreover, the dehydration of ettringite took place between 80°C and 150°C [52].

Moreover, according to Lothenbach's model [55], the higher the proportion of blast furnace slag in the cement mixture, the lower the quantity of ettringite in cement after hydration.

The first step in the dehydration process of the CSH gel occurred between the temperatures 180°C and 300°C [55].

As a result of the loss of bound water, the hydrated products turned into anhydrous products. It should be noted that the dehydration of the system leads to higher porosity and permeability. In addition, it was shown that the amount of evaporable water depends on the content of CSH gels present in the system. According to Richardson [63, 64], the amount of this water depends directly on its calcium-to-silica (C/S) ratio. Indeed, this quantity decreases with the (C/S) ratio. It should be noted that the pozzolanic reaction, due to the presence of blast furnace slag in CEMIII cement, produces CSH phases that give lower (C/S) ratios than in CEMI Portland cement. As a result, concrete (BIII) has less bound water in each CSH phase, and will therefore have less water to lose between 180°C and 300°C in comparison with concrete (BI).

Furthermore, microcracks are also responsible for increasing the permeability of concrete. In this context, Piasta [65] showed that the first microcracks appear in Ca(OH)<sub>2</sub> concentration zones at temperatures around 300°C. Once again, according to Lothenbach's model [54], the higher the proportion of blast furnace slag in the cement mixture, the lower the quantity of Ca(OH)<sub>2</sub> in cement after hydration.

Likewise, from the temperature of 400°C, the decomposition of calcium silicate hydrate (CSH) was relatively continuous up to 600°C [56]. It is useful to recall that the dehydration of portlandite Ca(OH)<sub>2</sub> generally starts at that temperature [66]. During cooling, the cracking in the cementitious material may get worse due to the modification

of the microstructure of the cementitious materials [55]. Noumowé [67] noticed that quicklime expansion occurred during its hydration, which regenerated part of portlandite. This expansion plays a major role in the formation of cracks during cooling. Cooling-dominated cracking was significantly weakened in the case of concrete (BIII) which contained less portlandite as a result of the pozzolanic reaction. This explains the higher permeability rate in concrete (BI) in comparison with that in concrete (BIII).

The inconsistency between porosity and permeability results can be attributed to the fact that the permeability of concretes does not only depend on porosity; it also depends on tortuosity, specific surface area, pore size distribution, and pore connectivity [68]. According to Delhomme [69], the pores that appear in mortars based on Portland cement, when exposed to high temperatures, are larger than those found in mortars made with blast furnace slag cement. In addition, it must be emphasized that enlarged pores are also a definite cause of increased permeability. Indeed, the sliding of gas molecules along the pore walls tends to be attenuated as the mean radius of pores becomes larger [70].

### 3.4 Capillary water absorption

Measuring capillary water absorption is a simple and easy technique to perform. This technique can be used to efficiently characterize the absorption kinetics of materials. It should also be noted that the higher the capillary absorption, the more quickly the material will be invaded by the liquids in contact. With regard to durability characterization, the most predominant element to be considered is of course the representative initial capillary water absorption. This is the amount of water absorbed per unit area, after one hour [46].

Figure 8 clearly illustrates the effect of temperature on the initial absorption, for the two types of cement used. It can be seen that the initial absorption increased as the temperature went up, for both types of concretes (BI and BIII).

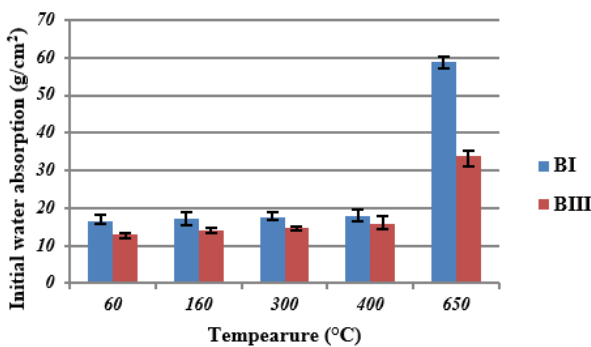


**Figure 8.** Effect of temperature on the initial water absorption of concrete

However, the increase rates in the initial absorption were greater in concretes (BIII) than in concretes (BI). For example, for concretes (BIII), the increase rates in the initial absorption were respectively equal to 10.20, 14.53, 24.19, and 162.77 % for the temperatures 160, 300, 400 and 650°C, against 4.19, 6.35, 8.25 and 254.09 % for concrete (BI), for the same temperatures.

Furthermore, it was also found that, for all the temperatures under consideration, the initial absorption of concretes (BIII) was always lower than that of concrete (BI). For example, at the reference temperature (60°C), the initial absorption of

concrete (BIII) was equal to 12.85 g/cm<sup>2</sup>, while it was 16.63 g/cm<sup>2</sup> for concrete (BI). Moreover, it was also shown that the decline in capillary water absorption was mainly due to the capillary porosity reduction, which contradicts the results about concrete porosity at this same temperature. It is widely admitted that water absorption capacity does not only depend on capillary porosity, but also on capillary pressure which is related to pore size, according to Jurin's law [71]. Obviously, the filling of a capillary pore is faster the larger its diameter [72]. In addition, the larger the diameter of a capillary pore, the faster it fills up. According to Jiang Shi-Ping and Grandet [73], the volume of large pores, for the same total porosity, is lower in blast furnace slag cement mortars than in Portland cement mortars. The positive effect of slag on reducing the water absorption of concrete has widely been mentioned in the literature [19, 32]. Several authors justified this improvement by the presence of calcium silicate hydrate (CSH) gel that is produced by the pozzolanic reaction of slag and also by the modification of the size distribution of the capillary pores [4].

For the other temperatures, the increase in initial absorption was generally attributed to the increase of porosity with temperature. In addition, between the temperatures 160°C and 300°C, the main factor causing the increase in pore sizes was the expansion of large capillaries as a result of the destruction of paste particles which served as walls of pores, and also the fusion of small pores [67, 74]. Beyond the temperature of 400°C, and particularly above 650°C, the change in porosity was due to the expansion of pores or to the formation of micro cracks [67, 74].

### 3.5 Diffusion of chloride ions

The binding capacity of chloride ions by the cement matrix constituents is an essential factor in transport kinetics. Indeed, in addition to their ability to modify the microstructure of the cement paste, the chemically and physically bound chlorides can retard the diffusion of chloride ions and decrease the quantity of free chlorides in the interstitial solution of pores. It was found that free chloride ions are the most harmful as they are responsible for the corrosion of concrete reinforcements.

The apparent diffusion coefficients of chloride ions for both types of concrete and for the different heating temperatures are clearly reported in Table 4 and Figure 9. Indeed, one can easily notice that, for both concretes (BI and BIII), the apparent diffusion coefficient (ADC) increased as the temperature augmented. This ADC increase may be explained by the chloride ion movement through the microcracks that developed on the surface of concrete as a result of the dehydration of cement paste and the decomposition of the hydration products of the cement after exposure to high temperatures and by the increase in capillary water absorption with increasing temperature, as previously suggested. Indeed, the penetration of chlorides into concrete is the result of complex physicochemical processes, in some cases coupling diffusion with capillary absorption or convection. We notice that for a mild increase in temperature, the ADC increases by 47 % and 34 %, respectively, for BI and BIII. However, for a more drastic increase in temperature, the ADC increases by 183 % and 126 %, respectively, for BI and BIII.

It can be said that, the ADCs do not increase with the same intensity. The rates of change in the apparent diffusion coefficient as a function of temperature were lower in concrete containing blast furnace slag cement (BIII) than in concrete including Portland cement (BI).

Furthermore, it is noted that for each temperature, the apparent diffusion coefficients of chloride ions in concretes (BIII) were significantly lower than those observed in concrete (BI), despite an often greater porosity. In addition, it should be noted that the water porosity, investigated in this study, remains a macroscopic parameter that does not give sufficient information on the structure of pores, unlike mercury porosimetry [75]. According to Shafikhani and Chidiac [76], in addition to porosity, the diffusion coefficient of chlorides depends on the tortuosity of hydrated cementitious materials which becomes more complex and longer. It is important to note that this decrease in diffusion coefficients of chloride ions is mainly due to the great tortuosity observed in the slag cement paste. According to Ortega et al. [77] and Hatanaka et al. [78], the tortuosity of slag-blended cement paste is higher than that of Portland cement-based paste. Therefore, the ion diffusion path would become longer after partial replacement of cement with slag. Li and Roy [79] also proposed an explanation concerning the reduction of chloride diffusivity in concrete due to the introduction of mineral admixture. They stated that since the potential hydraulicity and pozzolanic reaction not only fill up large pores but also reduce the pore connectivity and increase the tortuosity of pore, mineral admixtures lengthen the diffusion path of chloride.

The improved resistance to chloride ion diffusion in blast furnace slag concretes can also be attributed to the chemical and / or physical binding capacity of chlorides. Some chlorides can bond chemically with anhydrous products (C<sub>3</sub>A) which have not reacted during the ripening phase to form new chloride-based compounds (hydrated calcium monochloroaluminates such as Friedel's salt or hydrated calcium trichloroaluminate) [80]. According to Suryavanshi and Scantlebury [81], Friedel salts are formed by two distinct mechanisms: adsorption or ion exchange. In the latter case, the formation of the new chloride-based compound is explained by an exchange mechanism between a chloride ion (Cl<sup>-</sup>) from the interstitial solution and a hydroxide ion (OH<sup>-</sup>) intercalated in the AFm sheets (C<sub>4</sub>AH<sub>13</sub>). The hydroxide ion (OH<sup>-</sup>) being free to move easily, the chloride ion (Cl<sup>-</sup>) then replaces the hydroxide ion (OH<sup>-</sup>) in the intersheet spaces thus ensuring the electroneutrality of the system. In the case of adsorption, chlorides from the interstitial solution bind to the structure of the AFm phase ([Ca<sub>2</sub>Al(OH)<sub>6</sub>.2H<sub>2</sub>O]<sup>+</sup>) to rebalance the system's charges, which have been modified by the replacement of a calcium ion (Ca<sup>2+</sup>), by an aluminum ion (Al<sup>3+</sup>). In this context, Byfors [82] and Arya et al. [83] indicated that the C<sub>3</sub>A content has very little influence on the binding capacity of the hydrated cement paste. Rasheeduzzafar et al. [84] suggested that this is certainly due to the reaction of C<sub>3</sub>A with all the sulphates available during hydration. In this case, the major part of the C<sub>3</sub>A will have already reacted with the sulphates and there will hardly be any C<sub>3</sub>A left to react with the chlorides.

**Table 4.** Apparent diffusion coefficient of chloride ions as a function of temperature

Temperature [°C]	Apparent Diffusion Coefficient [10 <sup>-11</sup> m <sup>2</sup> /s]	
	BI	BIII
60	2.66	2.36
160	3.92	3.17
300	4.61	3.56
400	5.71	3.94
650	7.55	5.35

Consequently, this hypothesis should be rejected. Some researchers [85, 86] claimed that in addition to their chemical bonding with the aluminous phase of concrete, a significant amount of chlorides bind to the CSH gel which exists in large proportion in cement materials containing blast furnace slag. For example, Baroghel-Bouny [86] showed that the proportion of fixed chlorides can be quite high even in materials containing very little C<sub>3</sub>A and C<sub>4</sub>AF. These same researchers indicated that these ions can be physically adsorbed onto the surface of hydration products if there are positive adsorption sites on the negatively charged hydrates. They can also be incorporated into the structure of CSH clusters as calcium silicate hydrates are found in the form of sheets where chloride ions could be trapped [85]. To this end, Richardson [87] indicated that the calcium silicate hydrates that have an acicular (directional) morphology are gradually replaced by those exhibiting a sheet-like morphology when cement is partially replaced by blast furnace slag, which could justify the decrease in the diffusion coefficient in concrete incorporating blast furnace slag.

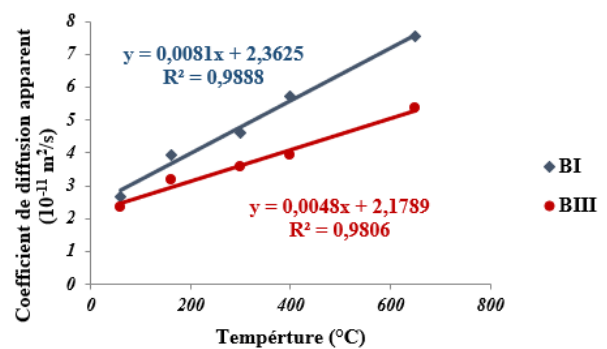


**Figure 9.** Effect of temperature on the diffusion coefficient of chloride ions in concrete

### 3.6 Correlation

It was deemed important to study the correlation between the apparent diffusion coefficient of chloride ions and the porosity accessible to water, initial water absorption, and gas permeability of concrete specimens, with and without blast furnace slag, for the purpose of better understanding the relationships between concrete properties that were measured in this study. Figure 10 clearly illustrates the relationships between the apparent diffusion coefficient and porosity (a), water absorption (b) and gas permeability (c).

Based on the results of the correlation coefficients and the correlation trends shown in Figure 10, it appears that the interrelationships between the apparent diffusion coefficient and sustainability indicators are influenced by the type of cement used. For example, a linear correlation was observed between the apparent diffusion coefficient and porosity (Figure 10(a)). However, the correlation coefficient measured on Portland cement-based concretes (BI) was relatively low ( $R^2 = 0.42$ ) given that the results obtained showed a greater dispersion. However, the correlation coefficient measured on concrete (BIII) including blast furnace slag was closer to unity ( $R^2 = 0.99$ ), which suggests the existence of a good correlation between the diffusion coefficient and porosity in the case of concrete (BIII). Further, Figure 10(b) shows the relationship between the initial water absorption and the chloride ion diffusion coefficient. It can clearly be observed that the chloride ion diffusion coefficient increased linearly with water

absorption for both types of concrete (BI and BIII). It is worth indicating that the concrete sample with the lowest absorption showed better resistance to chloride ion diffusion. In addition, the correlation coefficients ( $R^2$ ) were found to be equal to 0.96 and 0.97, respectively, for concrete with Portland cement (BI) and for that containing blast furnace slag cement (BIII), which implies that a good correlation exists between water absorption and chloride ion diffusion coefficient, regardless of the type of cement used. Regarding the relationship between the apparent chloride ion diffusion coefficient and gas permeability (Figure 10(c)), unlike the other two durability indicators, a logarithmic correlation was observed between permeability and diffusivity. However, the correlation between the apparent chloride ion diffusion coefficient and gas permeability was better in Portland cement-based concrete (BI); the correlation coefficient was closer to unity ( $R^2 = 0.92$ ). However, this correlation in concrete (BIII) containing blast furnace slag cement was lower; its correlation coefficient was found equal to  $R^2 = 0.74$ .

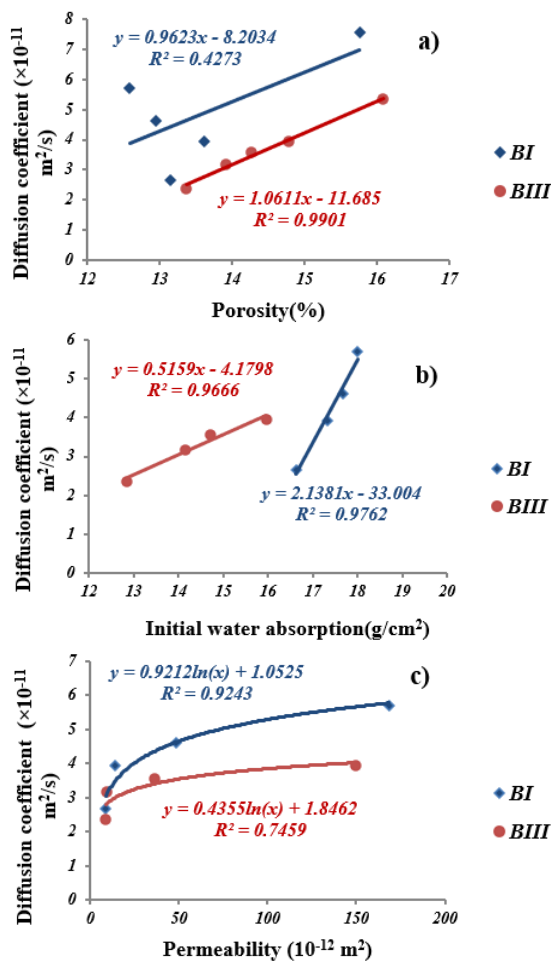


**Figure 10.** Correlations between the apparent diffusion coefficient and porosity (a), initial water absorption (b), and gas permeability (c)

#### 4. CONCLUSION

The effects of elevated temperatures on the physical and transfer properties of concrete containing blast furnace slag as a cementitious material were investigated in this study. The mass loss, porosity, capillary water absorption coefficient, permeability coefficient and chloride ion diffusion coefficient

of concrete were studied. In view of the results obtained in this study, the following conclusions can be drawn:

- The loss of mass increases progressively as the temperature augmented in both types of concrete (BI and BIII). However, the mass loss of concrete (BIII) incorporating blast furnace slag was higher than that of concrete (BI) containing Portland cement.
- At the temperatures 160°C and 650°C, the porosity of concrete (BI) increased, respectively, by 3.5 % and 19.8 %, while it decreased by 1.4 % and 4.3 %, respectively, at the temperatures 300°C and 400°C. On the other hand, porosity showed a linear increase in concrete (BIII). Indeed, the porosity of this type of concrete increased by 4.2 %, 6.6 %, 10.5 % and 20.3 %, respectively, for temperatures 160°C, 300°C, 400°C and 650°C.
- An exponential increase in the apparent permeability coefficient, and a linear increase in the apparent diffusion coefficient, were recorded for both types of concrete (BI and BIII) as the temperature was raised.
- The rate of change of gas permeability coefficient and diffusion of chloride ion coefficient with temperature was lower in concrete (BIII) than in concrete (BI).
- The initial water absorption increased when both types of concrete (BI and BIII) were exposed to high temperatures. However, it should be noted that the rates of increase of water absorption in concrete (BIII) were higher than those in concrete (BI).
- The initial water absorption of concretes (BIII) was lower than that of concrete (BI) for all the temperatures considered in this study.
- The apparent diffusion coefficient exhibited linear correlations with porosity and water absorption. However, there was a logarithmic relationship between the apparent diffusion coefficient and permeability.

This investigation developed some important data on the properties of concrete exposed to elevated temperatures up to 650°C. Indeed, based on the aforementioned point, there are benefits of replacing Ordinary Portland Cement with slag cement, such as improved resistance to the diffusion of chloride ions, capillary water absorption capacity, and gas permeability reduced.

We suggest that slag cement should be used to be a way of improving the durability of structures submitted to high temperatures or fire during their service life.

#### ACKNOWLEDGMENT

This study was conducted in Laboratory of Civil Engineering and Mechanical Engineering (LGCGM) of INSA-Rennes and the financial support rendered by the General Directorate for Scientific Research and Technological Development of Algeria. I thank Mrs. Siham Kamali-Bernard for welcoming me to this laboratory.

#### REFERENCES

- [1] Schneider, U. (1988). Concrete at high temperatures: A general review. *Fire Safety Journal*. 13: 55-68. [https://doi.org/10.1016/0379-7112\(88\)90033-1](https://doi.org/10.1016/0379-7112(88)90033-1)
- [2] Ulm, F.-J., Acker, P., Lévy, M. (1999). The Chunnel Fire. II: Analysis of concrete damage. *Journal of Engineering*



- Mechanics. 125(3): 283-289. [https://doi.org/10.1061/\(ASCE\)0733-9399](https://doi.org/10.1061/(ASCE)0733-9399)
- [3] Anderberg, Y. (1997). Spalling phenomena of HPC and OC. In NIST Workshop on Fire Performance of High Strength Concrete in Gaithersburg. North Capitol, WA, USA: US Government Printing Office.
- [4] Siddique, R., Kaur, D. (2012) Properties of concrete containing ground granulated blast furnace slag (GGBFS) at elevated temperatures. *Journal of Advanced Research*, 3: 45-51. <https://doi.org/10.1016/j.jare.2011.03.004>
- [5] Kodur, V. (2014). Properties of concrete at elevated temperatures. *ISRN Civil Engineering*, Hindawi Publishing Corporation. <https://doi.org/10.1155/2014/468510>
- [6] Sedaghatdoost, A., Behfarnia, K., Bayati M., Vaezi, M. (2019). Influence of recycled concrete aggregates on alkali-activated slag mortar exposed to elevated temperatures. *Journal of Building Engineering*, 26: 100871. <https://doi.org/10.1016/j.job.2019.100871>
- [7] Tufail, M. (2017). Effect of elevated temperature on mechanical properties of limestone, quartzite and granite concrete. *International Journal of Concrete Structures and Materials*, 11(1): 17-28. <https://doi.org/10.1007/s40069-016-0175-2>
- [8] Ercolani, G., Ortega, N.F., Priano, C., Señas, L. (2017). Physical-mechanical behavior of concretes exposed to high temperatures and different cooling systems. *Structural Concrete*. 18(3): 487-495. <https://doi.org/10.1002/suco.201500202>
- [9] Ashkezari, G.D., Razmara, M. (2020). Thermal and mechanical evaluation of ultra-high performance fiber-reinforced concrete and conventional concrete subjected to high temperatures. *Journal of Building Engineering*, 32: 101621. <https://doi.org/10.1016/j.job.2020.101621>
- [10] Abed, M., de Brito, J. (2020). Evaluation of high-performance self-compacting concrete using alternative materials and exposed to elevated temperatures by non-destructive testing. *Journal of Building Engineering*, 32: 101720. <https://doi.org/10.1016/j.job.2020.101720>
- [11] Pliya, P., Hajiloo, H., Romagnosi, S., Cree, D., Sarhat S., Green, M.F. (2021). The compressive behaviour of natural and recycled aggregate concrete during and after exposure to elevated temperatures. *Journal of Building Engineering*, 38: 102214. <https://doi.org/10.1016/j.job.2021.102214>
- [12] Jacobsen, S., Marchand, J., Gérard, B. (1998) *Concrete crack I: Durability and self-healing*. E&FN Spon, Concrete under severe conditions, 2: 217-231.
- [13] Darquennes, A., Olivier, K., Benboudjema F., Gagné, R. (2016). Self-healing at early-age, a way to improve the chloride resistance of blast furnace slag cementitious materials. *Construction and Building Materials*. 113: 1017-1028. <https://doi.org/10.1016/j.conbuildmat.2016.03.087>
- [14] Bijen, J. (1998). Blast furnace slag cement for durable marine structures. in: CIP Royal, Stichting Beton Prisma, The Netherlands.
- [15] Johari Megat, M.A., Brooks, J.J., Shahid, K., Rivard, P. (2011). Influence of supplementary cementitious materials on engineering properties of high strength Concrete. *Construction and Building Materials*. 25(5): 2639-2648. <https://doi.org/10.1016/j.conbuildmat.2010.12.013>
- [16] Bur, N. (2011). Pore structure of mortar Influence of cement base and curing. *European Journal of Environmental and Civil Engineering*, 15(5): 699-714. <https://doi.org/10.1080/19648189.2011.9693359>
- [17] Aghaeipour, A., Madhkhan, M. (2017). Effect of ground granulated blast furnace slag (GGBFS) on RCCP durability. *Construction and Building Materials*, 141: 533-541. <https://doi.org/10.1016/j.conbuildmat.2017.03.019>
- [18] Ortega, J.M., Sánchez, I., Climent, M.A. (2012). Durability related transport properties of OPC and slag cement mortars hardened under different environmental conditions. *Construction and Building Materials*, 27: 176-183. <https://doi.org/10.1016/j.conbuildmat.2011.07.064>
- [19] Hadj-Sadok, A., Kenai, S., Courard, L. Michel, F. Khatib, J. (2012). Durability of mortar and concretes containing slag with low hydraulic activity. *Cement and Concrete Composites*, 34: 671-677. <https://doi.org/10.1016/j.cemconcomp.2012.02.011>
- [20] Page, C.L., Short, N.R., El Tarras, A. (1981). Diffusion of Chloride ion in hardened cement pastes. *Concrete Research*, 11: 395-406. [https://doi.org/10.1016/0008-8846\(81\)90111-3](https://doi.org/10.1016/0008-8846(81)90111-3)
- [21] Szcześniak, A., Zychowicz, J., Stolarski, A. (2020). Influence of fly ash additive on the properties of concrete with slag cement. *Materials*, 13: 3265. <https://doi.org/10.3390/ma13153265>
- [22] Perlot, C., Verdier, J., Carcassès, M. (2006). Influence of cement type on transport properties and chemical degradation: Application to nuclear waste storage. *Materials and Structures*, 39: 511-523. <https://doi.org/10.1617/s11527-005-9020-9>
- [23] Hadj-sadok, A., Kenai, S., Courard, L., Darimont, A. (2011). Microstructure and durability of mortars modified with medium active blast furnace slag. *Construction and Building Materials*, 25: 1018-1025. <https://doi.org/10.1016/j.conbuildmat.2010.06.077>
- [24] Kim, S., kim, Y., Usman, M., Park, C., Hanif, A. (2021). Durability of slag waste incorporated steel fiber-reinforced concrete in marine environment. *Journal of Building Engineering*, 33: 101641. <https://doi.org/10.1016/j.job.2020.101641>
- [25] Wang, C., Wang, Y., Meng, Z. (2020). Resistance to chloride ion permeability of concrete mixed with fly ash, slag powder and silica fume. *Annales de Chimie-Science des Matériaux*, 44(1): 67-72. <https://doi.org/10.18280/acsm.440109>
- [26] McCaffrey, R. (2002). Climate Change and the Cement Industry, Environmental overview. GCL Magazine, environmental special issue. London, UK: Cement Trends.
- [27] Benhelal, E., Zahedi, G., Shamsaei, E., Bahadori, A. (2013). Global strategies and potentials to curb CO<sub>2</sub> emissions in cement Industry. *Journal of Cleaner Production*, 51: 142-161. <https://doi.org/10.1016/j.jclepro.2012.10.049>
- [28] Collins, F.G., Sanjayan, J.G. (1999). Workability and mechanical properties of alkali activated slag concrete. *Cement & Concrete Research*, 29(3): 455-458. [https://doi.org/10.1016/S0008-8846\(98\)00236-1](https://doi.org/10.1016/S0008-8846(98)00236-1)
- [29] Boukendakdji, O., Kadri, E.H., Kenai, S. (2012). Effects of granulated blast furnace slag and superplasticizer type on the fresh properties and compressive strength of self-compacting concrete. *Cement & Concrete Composites*,

- 34(4): 583-590. <https://doi.org/10.1016/j.cemconcomp.2011.08.013>
- [30] Oner, A., Akyuz, S. (2007). An experimental study on optimum usage of GGBS for the compressive strength of concrete. *Cement & Concrete Composites*, 29: 505-514. <https://doi.org/10.1016/j.cemconcomp.2007.01.001>
- [31] Boualleg, S. (2021). The study of lag cement's microstructural properties. *Annales de Chimie - Science des Matériaux*, 45(2): 121-133. <https://doi.org/10.18280/acsm.450204>
- [32] Güneyisi, E., Gesoğlu, M. (2008). A study on durability properties of high-performance concretes incorporating high replacement levels of slag. *Construction and Building Materials*, 41: 479-493. <https://doi.org/10.1617/s11527-007-9260-y>
- [33] ACI Committee. (1967). *Cement and concrete terminology: A glossary of terms in the field of cement and concrete technology*. American Concrete Institute.
- [34] Neville, A.M. (2004). *Properties of Concrete*. Pearson Prentice Hall, Essex.
- [35] Codina, M. (2007). *Les bétons bas pH: Formulation, caractérisation et étude long terme*. Ph.D. dissertation, INSA Toulouse, France. <https://theses.hal.science/tel-00199021/>.
- [36] Allahverdi, A., Maleki, A., Mahinroosta, M. (2018). Chemical activation of slag-blended Portland cement. *Journal of Building Engineering*, 18: 76-83. <https://doi.org/10.1016/j.jobe.2018.03.004>
- [37] NF EN 197-1. (2001). *Ciment, Partie 1: Composition, spécifications et critères de conformité des ciments courants*. Comité européen de normalisation.
- [38] Li, Q., Li, Z., Yuan, G. (2012). Effects of elevated temperatures on properties of concrete containing ground granulated blast furnace slag as cementitious material. *Construction and Building Materials*, 35: 687-692. <https://doi.org/10.1016/j.conbuildmat.2012.04.103>
- [39] Khan, M.S., Abbas, H. (2015). Performance of concrete subjected to elevated temperature. *European Journal of Environmental and Civil Engineering*, 20(5): 532-543. <https://doi.org/10.1080/19648189.2015.1053152>
- [40] Lubl6y, ., Kopecsk6, K., Bal6z, G.L., Szil6gyi, I.M., Madar6sz, J. (2016). Improved fire resistance by using slag cements. *Journal of Thermal Analysis and Calorimetry*, 125: 271-279. <https://doi.org/10.1007/s10973-016-5392-z>
- [41] TC-129-MHT. (1995). Rilem Technical Committees 129-MHT - test methods for mechanical properties of concrete at high temperatures. *Materials and Structures*, 28(181): 410-414.
- [42] AFPC-AFREM. (1997). *Determination de la masse volumique apparente et de la porositi accessible  l'eau. Methodes Recommandees Pour la Mesure des Grandeurs associees  la Durabilite*
- [43] RILEM TC 116-PCD. (1999). *Permeability of concrete as a criterion of its durability final report: Concrete durability-an approach towards performance testing*. *Materials and Structures*. 32(217): 163-173.
- [44] Koll k, J.J. (1989). The determination of the permeability of concrete to oxygen by the Cembureau method-a recommendation. *Materials and Structures*, 22: 225-230. <https://doi.org/10.1007/BF02472192>.
- [45] Attolou, A., Belloc, A., Torrenti, J.M. (1989). *Methodologie pour une nouvelle protection du beton vis--vis de la dessiccation*. *Bulletin des liaisons Ponts et Chaussees*, 164: 85-86.
- [46] Hall, C. (1989). Water sorptivity of mortars and concretes: A review. *Magazine of Concrete Research*, 41(147): 51-61. <https://doi.org/10.1680/mac.1989.41.147.51>
- [47] Nguyen, T.Q. (2007). *Modelisation physico-chimiques de la penetration des ions chlorures dans les materiaux cimentaires*. Ph.D. dissertation, ENPC, Paris, France.
- [48] Baroghel-Bouny, V., Belin, P., Maultzsch, M., Henry, D. (2007). AgNO<sub>3</sub> spray tests: Advantages, weaknesses, and various applications to quantify chloride ingress into concrete. Part 1: Non-steady-state diffusion tests and exposure to natural conditions. *Materials and Structures*, 40: 759-781. <https://doi.org/10.1617/s11527-007-9233-1>
- [49] Baroghel-Bouny, V., Belin, P., Maultzsch, M., Henry, D. (2007). AgNO<sub>3</sub> spray tests: Advantages, weaknesses, and various applications to quantify chloride. Part 2: Non-steady-state migration tests and chloride diffusion coefficients. *Materials and Structures*, 40: 783-799. <https://doi.org/10.1617/s11527-007-9236-y>
- [50] Kalifa, P., Tsimbrovska, M. (1998). *Comportement des BHP  hautes temperatures, tat de la question et resultats experimentaux*. *Cahier de CSTB*, 3078.
- [51] Noumowe, A., Siddique, R., Ranc, G. (2009). Thermo-mechanical characteristics of concrete at elevated temperatures up to 310C. *Nuclear Engineering and Design*, 239: 470-476. <https://doi.org/10.1016/j.nucengdes.2008.11.020>
- [52] Zhou, Q., Glasser, F.P. (2001). Thermal stability and decomposition mechanisms of ettringite at < 120C. *Cement & Concrete Research*, 31: 1333-1339. [https://doi.org/10.1016/S0008-8846\(01\)00558-0](https://doi.org/10.1016/S0008-8846(01)00558-0)
- [53] Chidiac, S.E., Panesar, D.K. (2008). Evolution of mechanical properties of concrete containing ground granulated blast furnace slag and effects on the scaling resistance test at 28 dabs. *Cement & Concrete Composites*, 30: 63-71. <https://doi.org/10.1016/j.cemconcomp.2007.09.003>
- [54] Lothenbach, B., Scrivener, K., Hooton, R.D. (2011). *Supplementary cementitious materials*. *Cement & Concrete Research*, 41(12): 1244-1256. <https://doi.org/10.1016/j.cemconres.2010.12.001>
- [55] Castellote, M., Alonso, C., Andrade, C., Turrillas, X., Campo, J. (2004). Composition and microstructural changes of cement pastes upon heating, as studied by neutron diffraction. *Cement & Concrete Research*, 34: 1633-1644. [https://doi.org/10.1016/S0008-8846\(03\)00229-1](https://doi.org/10.1016/S0008-8846(03)00229-1)
- [56] Bazant, Z.P., Kaplan M.F. (1996). *Concrete at high temperatures, material properties and mathematical models*. Longman House, Burnt Mill, England.
- [57] Divet, L., Le Roy, R. (2013). tude de la durabilite vis--vis de la corrosion des armatures des betons formules avec des ciments  forte teneur en laitier de haut fourneau. *Bulletin des Laboratoires des Ponts et Chaussees*, 280-281.
- [58] Piasta, J., Sawicz, Z., Rudzinski, L. (1984). Changes in the structure of hardened cement paste due to high temperature. *Materiaux et Construction*, 17(4): 291-296. <https://doi.org/10.1007/BF02479085>
- [59] Lion, M., Skoczylas, F., Lafhaj, Z., Sersar, M. (2005). Experimental study on a mortar. Temperature effects on porosity and permeability. Residual properties or direct measurements under temperature. *Cement & Concrete*

- Research, 35: 1937-1942. <https://doi.org/10.1016/j.cemconres.2005.02.006>
- [60] Sliwinski, J., Leonard, R., Tracz, T. (2004). Influence of high temperature on the residual permeability of high performance concrete (in Polish), Proceeding of 2nd Conference "Dni Betonu", Polski Cement, Wisła.
- [61] Choinska, M., Khelidj, A., Chatzigeorgiou, G., Pijaudier-Cabot, G. (2007). Effects and interactions of temperature and stress-level related damage on permeability of concrete. *Cement & Concrete Research*, 37: 79-88. <https://doi.org/10.1016/j.cemconres.2006.09.015>
- [62] Hui-sheng, S., Bi-wan, X., Xiao-Chen, Z. (2009). Influence of mineral admixtures on compressive strength, gas permeability and carbonation of high performance concrete. *Construction and Building Materials*, 23: 1980-1985. <https://doi.org/10.1016/j.conbuildmat.2008.08.021>
- [63] Richardson, I.G. (2000). The nature of the hydration products in hardened cement pastes. *Cement and Concrete Composites*, 22(2): 97-113. [https://doi.org/10.1016/S0958-9465\(99\)00036-0](https://doi.org/10.1016/S0958-9465(99)00036-0)
- [64] Richardson, I.G. (2008). The calcium silicate hydrates. *Cement & Concrete Research*, 38: 137-158. <https://doi.org/10.1016/j.cemconres.2007.11.005>
- [65] Piasta, J. (1984). Heat deformations of cement paste phases and the microstructure of cement paste. *Matériaux et Constructions*, 17(102): 415-420. <https://doi.org/10.1007/BF02473981>
- [66] Loukili, A., Khelidj, A., Richard, P. (1999). Hydration kinetics, change of relative humidity, and autogenous shrinkage of ultra-high-strength concrete. *Cement & Concrete Research*, 29: 577-584. [https://doi.org/10.1016/S0008-8846\(99\)00022-8](https://doi.org/10.1016/S0008-8846(99)00022-8)
- [67] Noumowé, A. (1995). Effet de hautes températures (20-600°C) sur le béton, Cas particulier du béton à hautes performances, Ph.D. dissertation, INSA Lyon, France.
- [68] Lafhaj, Z., Goueygou, M., Djerbi, A., Kaczmarek, M. (2006). Correlation between porosity, permeability and ultrasonic parameters of mortar with variable water/cement ratio and water content. *Cement and Concrete Research*, 36: 625-633. <https://doi.org/10.1016/j.cemconres.2005.11.009>
- [69] Delhomme, F., Ambroise, J., Limam, A. (2012). Effects of high temperatures on mortar specimens containing Portland cement and GGBFS. *Materials and Structures*, 45(11): 1685-1692. <https://doi.org/10.1617/s11527-012-9865-7>
- [70] Lion, M. (2004). Influence de la température sur le comportement poromécanique ou hydraulique d'une roche carbonatée et d'un mortier, études expérimentales. Ph.D. dissertation, École Centrale de Lille, France.
- [71] Jurin, J. (1718). An account of some experiments shown before the Royal Society; with an enquiry into the cause of the ascent and suspension of water in capillary tubes. *Philosophical Transactions of the Royal Society*, 30: 739-747. <https://doi.org/10.1098/rstl.1717.0026>
- [72] Balayssac, J.P., Detriche, C., Grandet, J. (1993). Intérêt de l'essai d'absorption d'eau pour la caractérisation du béton d'enrobage. *Materials and Structures*, 26: 226-230. <https://doi.org/10.1007/BF02472615>
- [73] Shi-Ping, J., Grandet, J. (1989). Évolution comparée des porosités des mortiers de ciment au laitier et des mortiers de ciment portland. *Cement & Concrete Research*, 19: 487-46. [https://doi.org/10.1016/0008-8846\(89\)90037-9](https://doi.org/10.1016/0008-8846(89)90037-9)
- [74] Tsimbrovska, M. (1998). Dégradation des bétons à hautes performances soumis à des températures élevées. Evolution de la perméabilité en liaison avec la microstructure, Ph.D. dissertation, University of Grenoble I, France.
- [75] Bajja, Z., Dridi, W., Darquennes, A., Bennacer, R., Le Bescop, P., Rahim, M. (2017). Influence of slurried silica fume on microstructure and tritiated water diffusivity of cement pastes. *Construction and Building Materials*, 132: 85-93. <https://doi.org/10.1016/j.conbuildmat.2016.11.097>
- [76] Shafikhani, M., Chidiac, S.E. (2019). Quantification of concrete chloride diffusion coefficient-A critical review. *Cement and Concrete Composites*, 99: 225-250. <https://doi.org/10.1016/j.cemconcomp.2019.03.011>
- [77] Ortega, J.M., Albaladejo, A., Pastor, J.L., Sánchez, I., Climent, M.A. (2013). Influence of using slag cement on the microstructure and durability related properties of cement grouts for micropiles. *Construction and Building Materials*, 38: 84-93. <https://doi.org/10.1016/j.conbuildmat.2012.08.036>
- [78] Hatanaka, A., Elakneswaran, Y., Kurumisawa, K., Nawa, T. (2017). The impact of tortuosity on chloride ion diffusion in slag-blended cementitious materials. *Journal of Advanced Concrete Technology*, 15: 426-439. <https://doi.org/10.3151/jact.15.426>
- [79] Li, S., Roy, D.M. (1986). Investigation of relations between volume of pore, pore structure and Cl-diffusion of fly ash and blended cement paste. *Cement & concrete research*, 16(5): 749-59. [https://doi.org/10.1016/0008-8846\(86\)90049-9](https://doi.org/10.1016/0008-8846(86)90049-9)
- [80] Ramachandran, V.S., Seeley, R.C., Polomark, G.M. (1984). Free and combined chloride in hydrating cement and cement compounds. *Materials and Structures*, 17: 285-289. <https://doi.org/10.1007/BF02479084>
- [81] Suryavanshi, A.K., Scantlebury, J.D. (1996). Mechanisme of friedel's salt formation in cements rich in tri-calcium aluminate. *Cement & Concrete Research*, 26(5): 717-727. [https://doi.org/10.1016/S0008-8846\(96\)85009-5](https://doi.org/10.1016/S0008-8846(96)85009-5)
- [82] Byfors, K. (1986). Chloride binding in cement paste. *Nordic Concrete Research*, 5: 27-38.
- [83] Arya, C., Buenfeld, N.R., Newman, J.B. (1990). Factors influencing chloride-binding in concrete. *Cement & Concrete Research*, 20: 291-300. [https://doi.org/10.1016/0008-8846\(90\)90083-A](https://doi.org/10.1016/0008-8846(90)90083-A)
- [84] Rasheeduzzafar, S., Hussain, E., Al-Saadoun, S.S. (1993). Effect of tricalcium aluminate content of cement on chloride binding and corrosion of reinforcing steel in concrete. *ACI Materials Journal*, 89(1): 3-12. <https://doi.org/10.14359/1239>
- [85] Beaudoin, J.J., Ramachandran, V.S., Feldman, R.F. (1990). Interaction of chloride and C-S-H. *Cement & Concrete Research*, 20: 875-883. [https://doi.org/10.1016/0008-8846\(90\)90049-4](https://doi.org/10.1016/0008-8846(90)90049-4)
- [86] Baroghel-Bouny, V., Chaussadent, T., Rharinaivo, A. (1995). Experimental investigations on binding of chloride in cementitious materials, in chloride penetration into concrete. Saint- Rémy-les-Chevreuses, France, RILEM.
- [87] Richardson, I.G. (1999). The nature of C-S-H in hardened cements. *Cement & Concrete Research*, 29: 1131-1147. [https://doi.org/10.1016/S0008-8846\(99\)00168-4](https://doi.org/10.1016/S0008-8846(99)00168-4)